Optical Materials 35 (2013) 1373–1377

Contents lists available at SciVerse ScienceDirect

Optical Materials

journal homepage: www.elsevier.com/locate/optmat

Effects of π-spacers on the linear and nonlinear optical properties of novel fluorenone-based D–π–A–π–D type conjugated oligomers with different donors

Tian-Hao Huang [a], Xue-Cong Li [a,b], Ying-Hui Wang [a,*], Zhi-Hui Kang [a], Ran Lu [c,*], Er-Long Miao [d] Fei Wang [d], Gao-Wen Wang [d], Han-Zhuang Zhang [a,*]

[a] College of Physics, Jilin University, Changchun 130012, China
[b] Department of Applied Physics, Tianjin Polytechnic University, Tianjin 300387, China
[c] College of Chemistry, Jilin University, Changchun 130012, China
[d] State Key Lab of Applied Optics, Changchun Institute of Optics, Fine Mechanics and Physics, Chinese Academy of Sciences, Changchun 130033, China

ARTICLE INFO

Article history:
Received 26 November 2012
Received in revised form 31 January 2013
Accepted 7 February 2013
Available online 13 March 2013

Keywords:
Fluorene–ethylene spacer
Two-photon absorption
z-Scan

ABSTRACT

We compare the effects of fluorene–ethylene (FE) spacers on the photo-physical properties of fluorenone-based conjugated oligomers. The introduction of FE spacer could modulate the steady-state spectra and weaken the difference between donor-dependent spectral features. Meanwhile, the quantum chemical calculations exhibit that the electron transition mechanism modulated by FE unit is variable with the donor of oligomers. The FE π-spacer mainly rises the HOMO and facilitates the electron delocalization in the fluorene end-capped oligomer, while it lowers the LUMO and enhances the donor effect in the triphenylamine end-capped one. The time-resolved fluorescence measurement exhibits that the difference between donor-dependent excited state lifetimes of oligomers becomes less obvious after the introduction of FE units. Moreover, the nonlinear optical measurements show that the FE spacer is able to improve the two-photon fluorescence efficiency and enhance the two-photon absorption cross-section of oligomers simultaneously, but the difference in two-photon characteristics between oligomers with different donors is also decreased.

1. Introduction

Two-photon absorption (TPA) is a nonlinear optical process in which two photons are absorbed simultaneously, exciting the molecules to a higher-energy state, with the energy being equal to the sum of the photon energies. Ever since, organic molecules with TPA behavior have attracted much attention due to their potential applications in 3D micro-fabrication and optical data storage [1–4], optical limiting [5,6], two-photon fluorescence microscopy [7] and photodynamic therapy [8], etc. Therefore, much effort has been devoted to the design and synthesis of molecules with large TPA cross-section. The π-conjugated oligomer is one of the important model molecules, which includes dipolar, quadrupolar, octupolar, and multipolar structures [9–11]. Among these structures, the quadrupolar D–π–A–π–D motif (D, A and π are electron donor, acceptor and bridge groups respectively) is highlighted due to its excellent TPA property [12]. Recently, people recognize that the TPA properties could depend on many other factors, such as the intramolecular charge transfer (ICT) character, the donor–acceptor strength, the molecular structure, and π-bridge groups [13,14]. Therefore, many linear conjugated oligomers have been synthesized with various π-conjugated spacers, donor or acceptor substituents [15–17]. Previous reports point out that the coplanarity of the π-conjugated spacers and the extension of π-system both improve the TPA cross-sections [18,19]. Moreover, the introduction of π-spacers is one of the most effective methods to simultaneously achieve the improvement of molecular coplanarity and π-system. Consequently, in order to understand the effect of π-spacers on the optical properties of linear conjugated oligomers in detail, we compare the photo-physical characteristics of four novel fluorenone-based oligomers (as seen in Fig. 1) in experimental and theoretical aspects. After the introduction of FE spacers between the terminal donor groups and the fluorenone core, we synthesized two new linear oligomers 2,7-di((*E*)-2-(7-((*E*)-2-(9,9-dioctyl-9*H*-fluoren-2-yl)vinyl)-9,9-dioctyl-9*H*-fluoren-2-yl)vinyl)-9-fluorenone (**F–F–FO–F–F**, #**3**) and 2,7-di((*E*)-2-(7-(4-(diphenylamino)styryl)-9,9-dioctyl-9*H*-fluoren-2-yl)vinyl)-9-fluorenone (**TPA–F–FO–F–TPA**, #**4**). In comparison with 2,7-di((*E*)-2-(9,9-dioctyl-9*H*-fluoren-2-yl)vinyl)-9-fluorenone (**F–FO–F**, #**1**) and 2,7-di(4-(diphenylamino)styryl)-9-fluorenone (**TPA–FO–TPA**, #**2**) as previously reported [20], the coplanarity and π-conjugated system of #**3** and #**4** have been obviously improved.

In this paper, we make a detailed comparison of the FE unit dependent photo-physical properties of oligomers with different donors by using of steady-state spectral measurements, time-cor-

* Corresponding authors. Tel.: +86 431 85167378; fax: +86 431 85166112 (H.-Z. Zhang).
E-mail addresses: yinghui_wang@jlu.edu.cn (Y.-H. Wang), luran@mail.jlu.edu.cn (R. Lu), zhanghz@jlu.edu.cn (H.-Z. Zhang).

0925-3467/$ - see front matter © 2013 Elsevier B.V. All rights reserved.
http://dx.doi.org/10.1016/j.optmat.2013.02.005

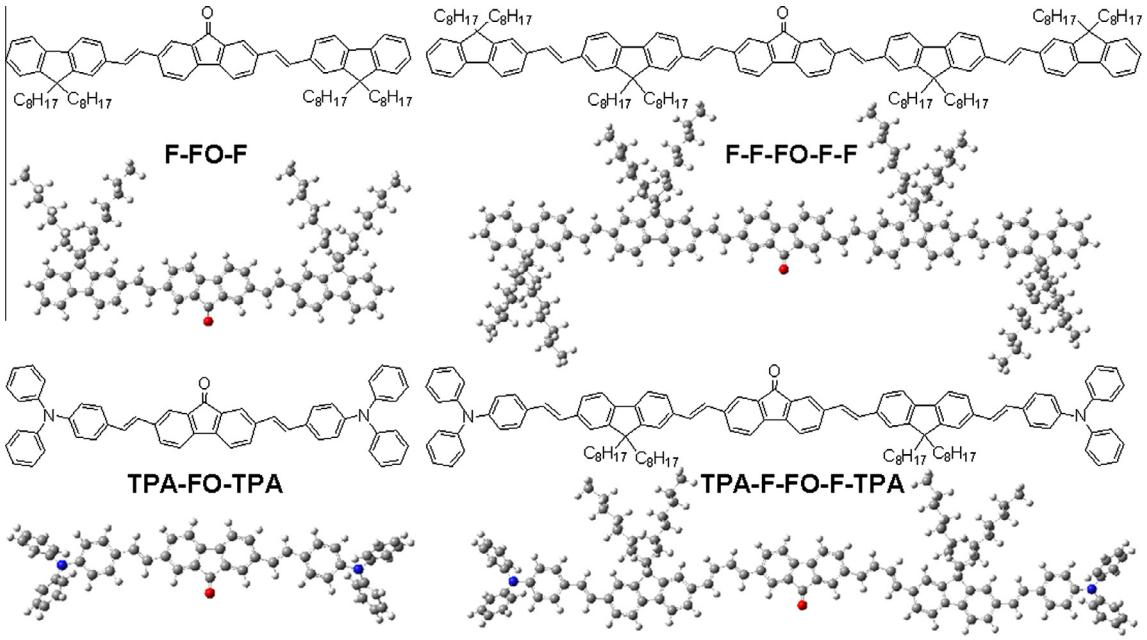

Fig. 1. Molecular structures of **F–FO–F** (#**1**), **TPA–FO–TPA** (#**2**), **F–F–FO–F–F** (#**3**) and **TPA–F–FO–F–TPA** (#**4**), together with their optimized ground state geometries as predicted by quantum chemical calculation.

related single-photon counting (TCSPC) technique, two-photon fluorescence (TPF) and femtosecond open aperture *z*-scan technique. Meanwhile, according to the quantum chemical calculation, we detailedly elaborate the electronic transition mechanism of oligomers, which is benefit for us to further understand the experimental results.

2. Materials and experimental measurements

All the oligomers were synthesized via Heck reaction [21], and the synthetic procedures of #**1** and #**2** have been reported in our previous work [20]. #**3** was obtained from **E-OFV2** [22] and 2,7-dibromo fluorenone following the general procedure for #**1**. The crude product was purified by column chromatography (silica gel, petroleum ether/dichloromethane 2:1) and recrystallized from ethanol/THF to give red powder. Yield: 68%. Mp: 144–146 °C. ^{1}H NMR (500 MHz, $CDCl_3$) δ 7.93 (s, 2H), 7.72–7.66 (m, 8H), 7.62 (d, J =7.0 Hz, 2H), 7.56–7.49 (m, 14H), 7.36–7.26 (m, 12H), 7.18 (d, J = 16.1 Hz, 2H), 2.08–1.96 (m, 16H), 1.21–1.04 (m, 80H), 0.82–0.78 (m, 24H), 0.72–0.61 (m, 16H). IR (KBr, cm^{-1}): 2955, 2925, 2853, 1711, 1635, 1464, 1385, 963, 881, 738. Elemental analysis calculated for $C_{137}H_{176}O$: C, 89.48; H, 9.65; O, 0.87. Found: C, 89.57; H, 9.56. MS, *m*/*z*: cal: 1838.9, found: 1838.6. #**4** was also synthesized following the similar procedure as that of #**1**. The crude product was purified by column chromatography (silica gel, petroleum ether/dichloromethane 7:2) and recrystallized from ethanol/THF to give orange–red powder. Yield: 70%. Mp: >200 °C. ^{1}H NMR (500 MHz, $CDCl_3$) δ 7.93 (s, 2H), 7.69–7.65 (m, 4H), 7.62 (d, J = 7.6 Hz, 2H), 7.50 (dd, J = 10.3, 7.6 Hz, 8H), 7.47–7.42 (m, 6H), 7.32–7.26 (m, 10H), 7.20–7.03 (m, 22H), 2.09–1.98 (m, 8H), 1.22–1.06 (m, 40H), 0.81 (t, J = 7.1 Hz, 12H), 0.70 (s, 8H). IR (KBr, cm^{-1}): 2956, 2925, 2854, 1719, 1457, 1385, 960, 880, 753. Elemental analysis calculated for $C_{115}H_{122}N_2O$: C, 89.21; H, 7.94; N, 1.81; O, 1.03. Found: C, 89.33; H, 7.86; N, 1.76. MS, *m*/*z*: cal: 1548.2, found: 1548.8.

Toluene solutions of all the oligomers were prepared at concentrations of 5×10^{-5} and 5×10^{-4} M, for linear and nonlinear optical measurements, respectively. Steady-state absorption spectra were measured using a UV–Vis spectrophotometer (Purkinje, TU-1810PC). One- and two-photon emission spectra were acquired using a fiber optic spectrometer (Ocean Optics, USB4000). Fluorescence dynamics at 600 nm was determined by a time-correlated single-photon counting spectrometer (Edinburgh, mini-τ), with an excitation wavelength of 405 nm (Edinburgh, EPL-405). Nonlinear optical measurements were performed using a mode-lock Ti:sapphire femtosecond laser system (Coherent), from where 2.2 mJ, 130 fs pulses at 800 nm with a repetition rate of 1 kHz can be obtained. The TPA cross-sections were measured by the femtosecond open aperture *z*-scan technique, details of the measurements have been reported before [20]. All optical measurements were carried out at room temperature, with the samples placed in a quartz cuvette (optical path: 2 mm).

3. Results and discussion

The steady-state absorption and one-photon fluorescence (OPF) spectra of these oligomers in toluene are shown in Fig. 2. All the oligomers show two obvious absorption features: the first absorption band (P_1) with lower intensity in the red region of the absorption spectra could be assigned to the ICT transition between the donor moieties and the fluorenone acceptor, while the second absorption peak (P_2) with higher intensity may be attributed to the π–π^* electronic transitions of the conjugated molecules [23]. As seen in Table 1, compared with #**1** and #**2**, the P_2 bands of #**3** and #**4** show red-shifts of 27 and 15 nm. Meanwhile, the P_1 and P_2 bands for #**2** show red-shifts of 13 and 17 nm, in comparison with those of #**1**. We can observe that the P_1 band of #**4** located around 500 nm is almost invariable, and the corresponding P_2 band is red-shifted only 5 nm as compared to those of #**3**. What's more, the molar absorption coefficients of #**3** and #**4** increase to 1.73×10^5 and 1.57×10^5 cm^{-1} M^{-1}, which are almost two times higher than those of #**1** (8.54×10^4 cm^{-1} M^{-1}) and #**2** (7.50×10^4 cm^{-1} M^{-1}), benefiting from the extension of π-conjugated system. In addition, the OPF intensity of oligomers bearing fluorene and triphenylamine donors obviously enhances after they are linked with the FE spacer. The emission peak of #**3** red-shifts

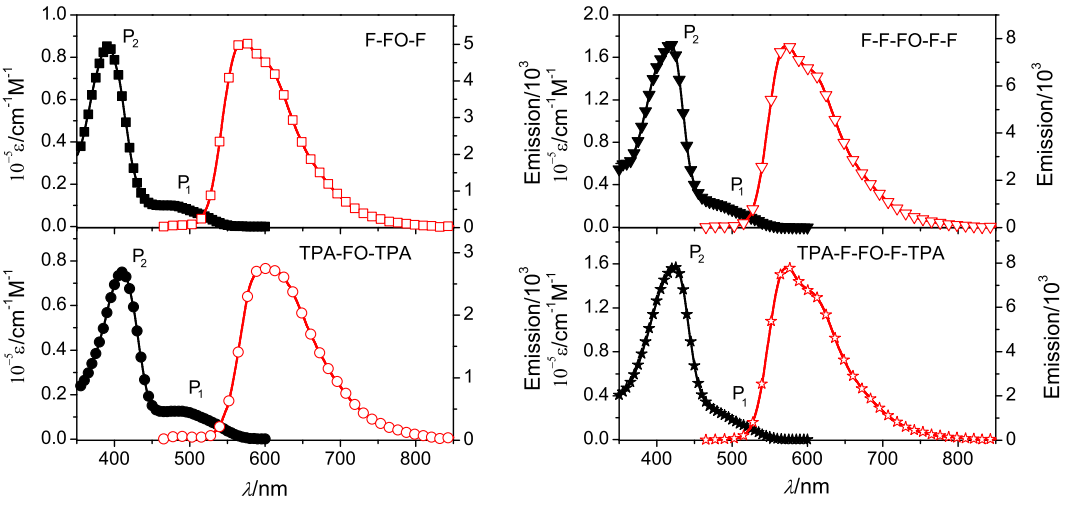

Fig. 2. Steady-state absorption and emission spectra of #**1**, #**2**, #**3** and #**4** in toluene (5.0×10^{-5} M).

Table 1
Photo-physical parameters of fluorenone-based linear conjugated oligomers.

Oligomers	F–FO–F	TPA–FO–TPA	F–F–FO–F–F	TPA–F–FO–F–TPA
λ_{abs}/nm	392	409	419	424
λ_{OPF}/nm	570	597	572	573
Stokes shift/nm	178	188	153	149
τ_f/ns	3.0	1.9	2.6	2.5
λ_{TPF}/nm	575	605	574	574
$\beta/10^{-2}$ cm GW^{-1}	0.76	1.07	1.89	2.13
$\sigma^{(2)}$/GM	626	884	1561	1759

about 2 nm, meanwhile that of #**4** shifts about 24 nm in the opposite direction. It is interestingly found that the emission peaks of #**3** and #**4** are almost at the same position of ~572 nm, even though they have different donors. We can also confirm that the Stokes shifts, given by the wavelength difference between the absorption and emission maximum of oligomers, obviously decrease from 178 (#**1**) to 153 (#**3**) nm, and from 188 (#**2**) to 149 (#**4**) nm. The difference of Stokes shift between #**3** and #**4** becomes further low and decreases from 10 to 4 nm by comparison to that between #**1** and #**2**.

In an effort to understand the π-spacer dependent optical and electronic properties of these linear conjugated oligomers at the molecular level, quantum chemical calculation based on DFT was used to calculate the electronic structures and investigate the ground to excited state transitions. Fig. 1 have shown the optimized ground state geometries of #**1**, #**2**, #**3** and #**4** obtained with the B3LYP [24]/3-21G basis set. Apparently, the introduction of π-spacer leads to the extension of π-conjugated system and is benefit for the delocalization of π-electron over the whole oligomers. Moreover, the coplanar conformation of molecules is sufficiently maintained by the introduction of FE spacer, which means that the coplanar π-spacer could further facilitate the π-electron delocalization.

The calculated HOMO and LUMO energy levels of #**1**, #**2**, #**3** and #**4** are summarized in Fig. 3. The HOMO levels for compounds #**3** and #**4** are −5.025 and −4.786 eV, respectively, and the LUMO levels for them are −2.429 and −2.480 eV. When FE spacer is introduced, for oligomers with fluorene donor, the LUMO is almost invariable (~0.017 eV), but the HOMO obviously rises ~0.184 eV. For the oligomers with triphenylamine donor, the HOMO varies a little (~0.061 eV), but the LUMO apparently decreases ~0.156 eV. Apparently, the molecular frontier orbitals could narrow the band gap of fluorene and triphenylamine end-capped oligomers, even though their origins are obviously different. FE spacer mainly rises the HOMO of fluorene end-capped oligomer, while lowers the LUMO of triphenylamine end-capped one.

Fig. 4 shows the plots of the representative molecular frontier orbitals in the ground states of #**3** and #**4**. In both oligomers, the LUMO levels are localized in the fluorenone moiety, but the distributions of HOMO levels have difference. The HOMO of #**3** is almost delocalized over the whole molecule, which is similar to that of #**1** [20], but that of #**4** mainly distributes in the triphenylamine and FE moieties and only a little part of it is localized in the fluorenone unit. The results indicate that the HOMO–LUMO transitions in both oligomers show a significant ICT character, which is in agreement with the steady-state spectra. The distributions of electron cloud further confirm that the effect of π-spacer on fluorene end-capped oligomer facilitates the electron delocalization, while that on triphenylamine end-capped oligomer could enhance the role of do-

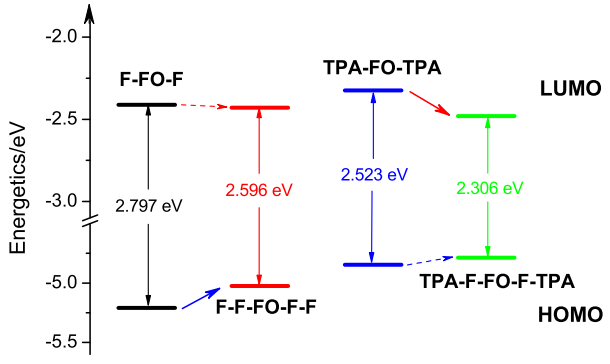

Fig. 3. Values of HOMO and LUMO for #**1**, #**2**, #**3** and #**4**.

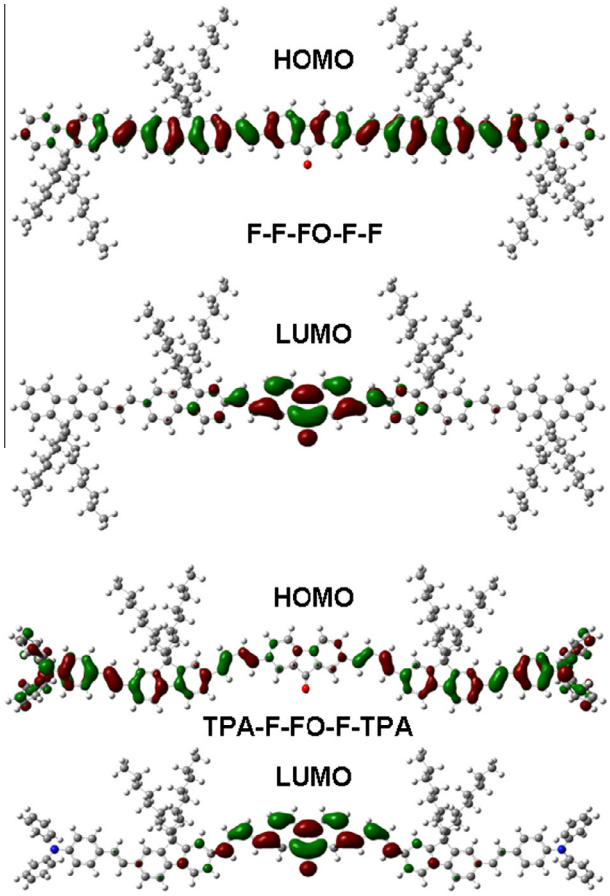

Fig. 4. HOMO and LUMO orbitals in the optimized ground state structure of #**3** and #**4**.

nor. Moreover, the π-spacer unit in #**4**, acting as a part of donor, could participate in the ICT transition. Even though the photophysical properties of oligomers with different donors are both enhanced obviously by introducing the FE spacer, and their difference in optical properties are weakened in a certain extent, the calculations confirm that their origins are much different. The DFT calculations on the four compounds discussed above provide deep insight into the variation of electronic structures and properties induced by the π-spacer unit.

The excited state lifetimes of these oligomers are measured by employing TCSPC technique, with an excitation wavelength at 405 nm. All the oligomers exhibit a mono-exponential decay as seen in Fig. 5, and the lifetime values can be obtained by fitting experimental data with a mono-exponential function. The lifetimes of #**1** and #**2** are 3.0 and 1.9 ns, respectively, and those of #**3** and #**4** are 2.6 and 2.5 ns respectively, which become similar to each other. In a word, the introduction of FE spacer could really improve the optical properties of oligomer, meanwhile weaken the difference between the oligomer with fluorene and that with triphenylamine donors simultaneously.

Similar to the previous report [20], we again observe the fluorescence emission of these oligomers under the excitation of femtosecond pulses at 800 nm, and the peak wavelengths are listed in Table 1. As shown in Fig. 6, the emission spectra of #**3** and #**4** show similar spectral behavior to that of the OPF spectra, implying that their emission mechanism may be much similar to the single photon transition. The insets show linear dependence of the integral fluorescence intensity on the square of the excitation energies, which again confirm that the TPA process should be responsible

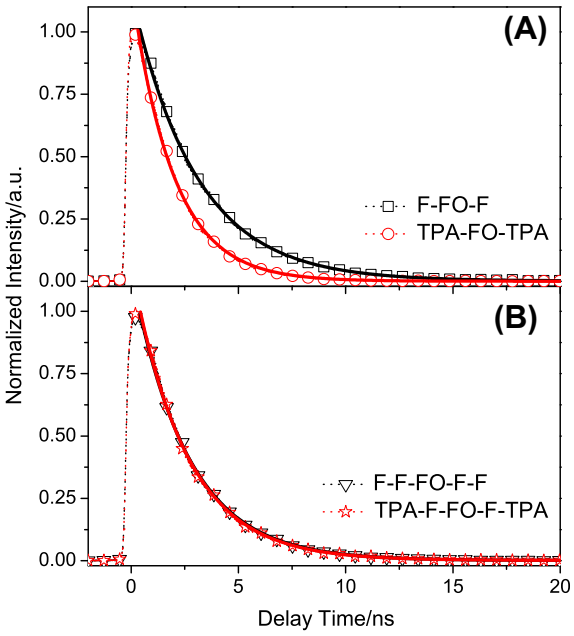

Fig. 5. Time-dependent fluorescence kinetics (dot lines) at 600 nm and mono-exponentially fitted lines (solid) of (A) #**1** and #**2** (B) #**3** and #**4** with a concentration of 5.0×10^{-5} M at the excitation wavelength of 405 nm.

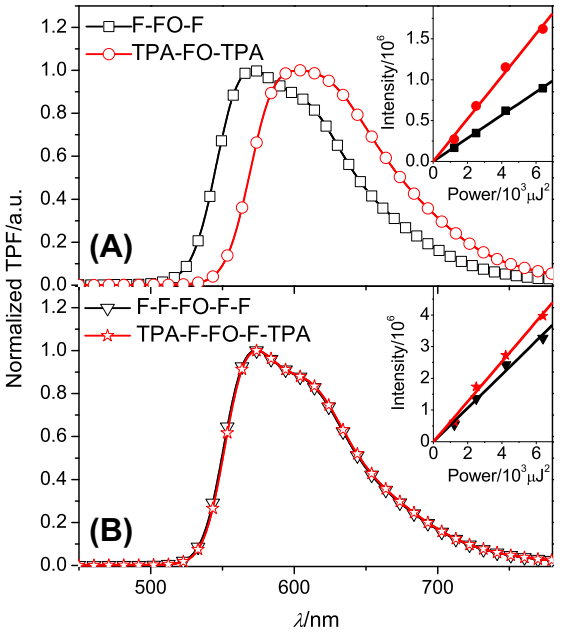

Fig. 6. Normalized two-photon fluorescence (TPF) spectra of (A) #**1** and #**2**; (B) #**3** and #**4** in toluene (5.0×10^{-4} M) excited by femtosecond laser pulses at 800 nm. Insets: the linear dependence of TPF intensity on the square of excitation power for (A) #**1** (solid square) and #**2** (solid circle); (B) #**3** (solid inverted triangle) and #**4** (solid star).

for the 800 nm excited fluorescence. As seen from the slope in the inset of Fig. 6, the TPF efficiency of #**3** and #**4** is 3.7 and 2.5 times higher than that of #**1** and #**2**, respectively, which is benefit from the extension of π-conjugated system. Additionally, we can also calculate that the ratio of TPF efficiency of #**2** to #**1** is 9:5, and that of #**4** to #**3** is 6:5, suggesting that the difference of TPF efficiency between #**3** and #**4** is obviously less than that between #**1** and #**2**.

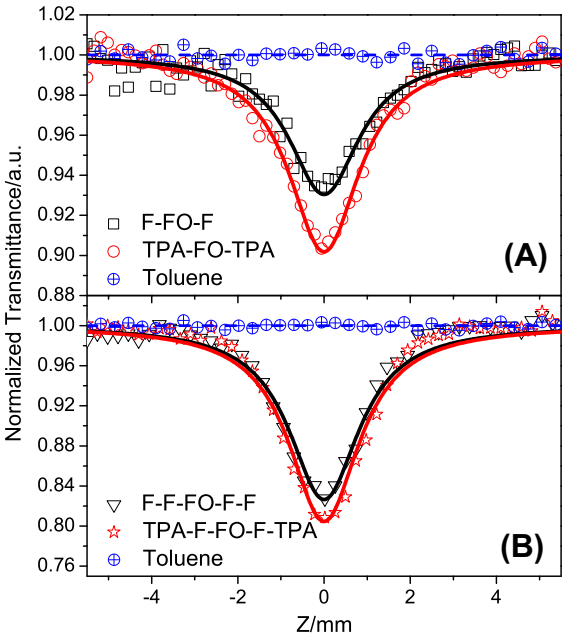

Fig. 7. Open aperture *z*-scan profiles and fitting lines (solid) for (A) #**1** and #**2**; (B) #**3** and #**4** in toluene (5.0×10^{-4} M), with the pulse energy of ~250 nJ.

Their TPA cross-sections have been further determined by using femtosecond open aperture *z*-scan technique at 800 nm. As seen in Fig. 7, we exclude the influence of the solvent nonlinearity by detecting the *z*-scan signature of neat toluene. The *z*-scan results for these oligomers in toluene are also shown in Fig. 7. The nonlinear absorption coefficient (β) and TPA cross-section ($\sigma^{(2)}$) can be calculated using the same method as described in our last work [20]. The obtained β and $\sigma^{(2)}$ values are summarized in Table 1. All the oligomers show considerable TPA cross-sections, and it is clearly seen that the TPA cross-sections of FE π-bridged oligomers are 2.5 and 2 times higher than their ethenylene π-bridged counterparts. This observation indicates that the introduction of FE spacer plays an important role in enhancing the TPA cross-section, due to the extension of π-conjugated system. As shown in our previous work, the TPA cross-section of #**2** (884 GM) is 1.4 times higher than that of #**1** (626 GM). However, when FE spacer is introduced, the $\sigma^{(2)}$ value of #**4** (1759 GM) is similar to that of #**3** (1561 GM, $\sigma^{(2)}$ is only 1.1 times smaller). Apparently, the FE π-spacer would enhance the TPA cross-section, at the same time as weakening the difference between donor-dependent oligomers. And this situation is similar to those in the linear optical measurements, indicating that the FE spacer could weaken the effect of donor units on the optical properties.

4. Conclusion

We have systematically compared the π-spacer dependent optical properties of novel fluorenone-based conjugated oligomers with different donors in detail. The FE spacer could modulate the steady-state spectral feature, increase the TPF efficiency and enhance the TPA cross-section due to the extended π-system. Meanwhile, the introduction of fluorene–ethylene (FE) spacer is able to narrow the difference in optical properties between oligomers with different donors. DFT calculations offer a better understanding of the π-spacer dependent electronic structures and properties, and show that the mechanisms responsible for the similar experimental optical features of the two FE π-bridged oligomers are different. This study could provide a useful guideline for the modulation and design of novel π-conjugated oligomers with enhanced TPA properties.

Acknowledgements

This work was supported by the National Natural Science Foundation of China (Nos. 10974071, 10774060, 21103161 and 11274142), the Jilin Province Natural Science Foundation of China (No. 20070512), the National Found for Fostering Talents of Basic Science (No. J1103202) and the China Postdoctoral Science Foundation (2011M500927). The calculations with the Gaussian 09 program were performed at the State Key Laboratory of Supramolecular Structure and Materials, Jilin University, China.

References

[1] D.A. Parthenopoulos, P.M. Rentzepis, Science 245 (1989) 843.
[2] S. Kawata, Y. Kawata, Chem. Rev. 100 (2000) 1777.
[3] S. Kawata, H.-B. Sun, T. Tanaka, K. Takada, Nature 412 (2001) 697.
[4] W. Zhou, S.M. Kuebler, K.L. Braun, T. Yu, J.K. Cammack, C.K. Ober, J.W. Perry, S.R. Marder, Science 296 (2002) 1106.
[5] C.W. Spangler, J. Mater. Chem. 9 (1999) 2013.
[6] M. Calvete, G.Y. Yang, M. Hanack, Synth. Met. 141 (2004) 231.
[7] M.C. Skala, J.M. Squirrel, K.M. Vrotsos, V.C. Eickhoff, A. Gendron-Fitzpatrick, K.W. Eliceiri, N. Ramanujam, Cancer Res. 65 (2005) 1180.
[8] D. Gao, R.R. Agayan, H. Xu, M.A. Philbert, R. Kopelman, Nano Lett. 6 (2006) 2383.
[9] B.A. Reinhardt, L.L. Brott, S.J. Clarson, A.G. Dillard, J.C. Bhatt, R. Kannan, L. Yuan, G.S. He, P.N. Prasad, Chem. Mater. 10 (1998) 1863.
[10] L. Ventelon, L. Moreaux, J. Mertz, M. Blanchard-Desce, Chem. Commun. 45 (1999) 2055.
[11] B.R. Cho, K.H. Son, S.H. Lee, Y.-S. Song, Y.-K. Lee, S.-J. Jeon, J.-H. Choi, H. Lee, M. Cho, J. Am. Chem. Soc. 123 (2001) 10039.
[12] S. Das, A. Nag, D. Goswami, P.K. Bharadwaj, J. Am. Chem. Soc. 128 (2006) 402.
[13] D. Beljonne, W. Wenseleers, E. Zojer, Z.G. Shuai, H. Vogel, S.J.K. Pond, J.W. Perry, S.R. Marder, J.-L. Brédas, Adv. Funct. Mater. 12 (2002) 631.
[14] H.M. Kim, M.S. Seo, S.-J. Jeon, B.R. Cho, Chem. Commun. 47 (2009) 7422.
[15] G. Qian, Z.Y. Wang, Can. J. Chem. 88 (2010) 192.
[16] F. Jaramillo-Isaza, M.L. Turner, J. Mater. Chem. 16 (2006) 83.
[17] A.R. Morales, K.D. Belfield, J.M. Hales, E.W. Van Stryland, D.J. Hagan, Chem. Mater. 18 (2006) 4972.
[18] O. Mongin, L. Porrès, M. Charlot, C. Katan, M. Blanchard-Desce, Chem. Eur. J. 13 (2007) 1481.
[19] J.-Z. Cheng, C.-C. Lin, P.-T. Chou, A. Chaskar, K.-T. Wong, Tetrahedron 67 (2011) 734.
[20] T.-H. Huang, D. Yang, Z.-H. Kang, E.-L. Miao, R. Lu, H.-P. Zhou, F. Wang, G.-W. Wang, P.-F. Cheng, Y.-H. Wang, H.-Z. Zhang, Opt. Mater. 35 (2013) 467.
[21] R.F. Heck, J.P. Nolley, J. Org. Chem. 37 (1972) 2320.
[22] H.P. Zhou, R. Lu, X. Zhao, X.P. Qiu, P.C. Xue, X.L. Liu, X.F. Zhang, Tetrahedron Lett. 51 (2010) 5287.
[23] S.A. Jenekhe, L.D. Lu, M.M. Alam, Macromolecules 34 (2001) 7315.
[24] C. Lee, W. Yang, R.G. Parr, Phys. Rev. B. 37 (1988) 785.